2013-12-01

Regulation of the Myostatin Protein in Overload-Induced Hypertrophied Rat Skeletal Muscle

Paige Abriel Affleck
Brigham Young University - Provo

Regulation of the Myostatin Protein in Overload-Induced Hypertrophied Rat Skeletal Muscle

Paige A. Affleck

A thesis submitted to the faculty of
Brigham Young University
in partial fulfillment of the requirements for the degree of

Master of Science

Gary W. Mack, Chair
Allen C. Parcell
David M. Thomson

Department of Exercise Sciences

Brigham Young University

December 2013

ABSTRACT

Regulation of the Myostatin Protein in Overload-Induced
Hypertrophied Rat Skeletal Muscle

Paige A. Affleck
Department of Exercise Sciences, BYU
Master of Science

Myostatin (GDF-8) is the chief chalone in skeletal muscle and negatively controls adult skeletal muscle growth. The role of myostatin during overload-induced hypertrophy of adult muscle is unclear. We tested the hypothesis that overloaded adult rodent skeletal muscle would result in reduced myostatin protein levels. Overload-induced hypertrophy was accomplished by unilateral tenotomy of the gastrocnemius tendon in male adult Sprague-Dawley rats followed by a two-week period of compensatory overload of the plantaris and soleus muscles. Western blot analysis was performed to evaluate changes in active, latent and precursor myostatin protein levels. Significant hypertrophy was noted in the plantaris (494 ± 29 vs. 405 ± 15 mg, $p < 0.05$) and soleus (289 ± 12 vs. 179 ± 37 mg, $p < 0.05$) muscles following overload. Overloaded soleus muscle decreased the concentration of active myostatin protein by 32.7 ± 9.4% ($p < 0.01$) while the myostatin precursor protein was unchanged. Overloaded plantaris muscle decreased the concentration of active myostatin protein by 28.5 ± 8.5% ($p < 0.01$) while myostatin precursor levels were reduced by 17.5 ± 5.9% ($p < 0.05$). Myostatin latent complex concentration decreased in the overloaded soleus and plantaris muscle by 15.0 ± 5.9% and 70.0 ± 2.3% ($p < 0.05$), respectively. These data support the hypothesis that the myostatin signaling pathway in overloaded muscles is generally downregulated and contributes to muscle hypertrophy. Plasma concentrations of total and active myostatin proteins were similar in overloaded and control animals and averaged 8865 ± 526 pg/ml and 569 ± 28 pg/ml, respectively. Tissue levels of BMP-1, an extracellular proteinase that converts myostatin to its active form, also decreased in overloaded soleus and plantaris muscles by 40.4 ± 12.9% and 32.9 ± 6.9% ($p < 0.01$), respectively. These data support the hypothesis that local, rather than systemic, regulation of myostatin contributes to the growth of individual muscles, and that an association exists between the extracellular matrix proteinase BMP-1 and the amount of active myostatin in overloaded muscles.

Keywords: myostatin, GDF-8, TGF-β superfamily, BMP-1/tolloid proteinases, BMP-1, mechanical overload, muscle growth, hypertrophy

TABLE OF CONTENTS

LIST OF FIGURES

INTRODUCTION

Myostatin is a growth and differentiation factor in the transforming growth factor-β (TGF-β) superfamily (24). The TGF-β superfamily encompasses the growth and differentiation factors responsible for embryonic development and maintaining tissue homeostasis in adults (24). Myostatin, also called growth and differentiation factor 8 (GDF-8), is predominantly expressed in human embryotic and mature adult skeletal muscle (24). Myostatin is involved in the regulation of muscle size due to its dual regulatory role: the regulation of the number of muscle fibers during development (hyperplasia) (19) and the regulation of postnatal muscle fiber growth (hypertrophy) (19, 34, 36).

Mutations in the myostatin gene (24, 25, 29) result in an inactive protein and increased muscle mass (aka "double muscling"). In humans and animals without this gene mutation, levels of the myostatin protein are variable and it acts in a concentration-dependent manner to negatively regulate muscle growth (19). Myostatin mRNA expression is decreased in most (28, 38), but not all (14), studies evaluating loading of adult skeletal muscle. However, only a handful of studies have measured active myostatin protein levels. These studies show that the concentrations of active myostatin protein decrease with aerobic exercise (12). In contrast, active myostatin protein levels have been shown to either increase or decrease with testosterone administration (15, 16), depending on the time course and age of subjects. Myostatin undergoes several posttranslational modifications before becoming an active molecule; thus it is possible that the regulation of posttranslational changes in myostatin account for the apparent discordance between myostatin gene expression and protein concentrations.

Myostatin is synthesized as a 376 amino acid precursor protein (24). The 52 kD precursor myostatin protein includes a 26 kD N-terminal dimer (propeptide), a 12.5 kD C-terminal (active

myostatin) dimer and a signaling peptide (24). The precursor protein must undergo proteolytic processing to be released from the cell and to become an active molecule (19, 22). Following proteolytic processing and secretion the mature myostatin (C-terminal dimer) remains non-covalently bound to the propeptide (N-terminal) in an inactive, latent complex (22, 30). This myostatin latent complex is thought to be available locally in the extracellular matrix (3) and also circulates in the blood (40). As long as the protein is in the latent complex, activity of the C-terminal dimer is blocked, and receptor binding of the protein does not occur (22, 30). Once the C-terminal dimer is proteolytically cleaved from the propeptide and thus activated, myostatin can bind to the activin type II receptor (either ActRIIA or ActRIIB) (31). Myostatin binding to the activin receptor initiates an intracellular signaling cascade involving SMAD2/SMAD3 (17, 27). These SMAD proteins act as intracellular mediators for myostatin signaling as well as regulate myostatin gene expression in a dose-dependent manner (19).

While altering the amount of myostatin in the precursor form is a first step in regulating active myostatin levels, the extracellular processing of the latent complex may be even more important. Several mechanisms are capable of latent myostatin cleavage such as: acid, alkali, heat, limited proteolysis and incubation by glycosidases (26, 40). The exact mechanism by which latent myostatin is activated *in vivo* is unclear; however, recent evidence indicates that BMP-1/tolloid proteinases in the extracellular matrix are capable of cleaving and activating the myostatin latent complex (5, 21, 37).

A reduction in myostatin mRNA expression is associated with conditions that favor muscle hypertrophy (35). However, reducing extracellular processing of the myostatin latent complex also promotes muscle hypertrophy (21). The purpose of this study was to create an overload condition in adult skeletal muscle and thereby induce a change in skeletal muscle

myostatin protein concentrations. We hypothesize that in overload-induced hypertrophy we will see decreased active myostatin muscle concentrations with little or no change in circulating active myostatin concentrations. We also hypothesize that the decrease in skeletal muscle active myostatin will be associated with a reduction in BMP-1 levels leading to reduced capacity to convert the latent myostatin complex into its active form. In addition, if extracellular processing by BMP-1 is an important component of this response we would expect the amount of myostatin latent complex in circulation and in the muscle to increase.

METHODS

Animals. Eleven adult male Sprague-Dawley (300-350 g) rats were used in this research study. Animals were housed individually in activity wheel cages (Lafayette Instrument Company, Lafayette, IN) in the animal care facility at Brigham Young University. They were kept on a 12 h dark-light cycle in a temperature-controlled environment (21-22°C). Rats were fed standard rat chow and water *ad libitum.* All experimental procedures and animal care protocols were approved by the Institutional Animal Care and Use Committee at Brigham Young University.

Experimental Design. A compensatory overload model was used to induce hypertrophy in the rodent skeletal muscle to examine myostatin signaling. The compensatory overload model was chosen because it produces significant and rapid hypertrophy within 1-6 d (6, 8, 10) as well as increased amino acid uptake (6, 9), and protein synthesis (7, 18) in the overloaded skeletal muscles. Animal wheel-running activity was measured 5 d prior to surgery. Each animal received a gastrocnemius tenotomy surgery on one hindlimb in a randomized fashion and the opposite hindlimb received a sham (control) surgery. After surgery, the animals were allowed to recover for 14 d while running wheel activity was monitored. After this overload period the

plantaris and soleus muscles of the tenotomized hindlimb were harvested (Treatment group: TEN, n = 11) as well as the plantaris and soleus muscles from the sham operated hindlimb (Control group: CON, n = 11). The harvested tissue was weighed, flash frozen, and stored at -80°C until analysis of myostatin and BMP-1 protein levels by Western blot occurred.

Wheel-Running Activity. Animal wheel-running activity was measured 5 d prior to surgery and during the entire 14-day overload period using Activity Wheel Monitoring Software (Lafayette Instrument Company, Lafayette, IN). Wheel-running totals were downloaded once every hour during dark cycles (awake) and once every 4 h during light (sleep) cycles. Running wheel activity was used to monitor running behavior pre- and postsurgery to ensure similar amounts of activity and thereby mechanical overload during the overload period.

Synergist Tenotomy Surgery. Overload-induced hypertrophy of the plantaris and soleus muscles was achieved with a unilateral tenotomy of the gastrocnemius tendon. Animals were given Rimadyl chewable tablets (5mg/kg body weight) 24 h prior to surgery and once every 24 h for 5 d following surgery. Animals were also administered a subcutaneous injection of buprenorphine (0.06 mg/kg body weight) immediately prior to surgery and every 6-12 h postsurgery for 48 h. At the start of surgery, animals were weighed, placed on a heating pad and anesthetized with 2-3% isoflurane and supplemental oxygen. Animals were anesthetized throughout the surgery and the depth of anesthesia was monitored with a pedal reflex. The skin on the posterior side of each hindlimb was shaved and cleaned with vetadine solution. Under sterile conditions, a 1 cm incision was made at the myotendinous junction of each hindlimb. The fascia surrounding the incision was separated using blunt dissection. The medial and lateral heads of the gastrocnemius were isolated, spliced and sutured back into the muscle belly in hindlimbs receiving a tenotomy surgery. In control hindlimbs, the gastrocnemius attachments

were isolated but remained intact to allow normal function of the gastrocnemius muscle during the overload period. All incisions were closed with two 9 mm MikRon stainless steel surgical clips. Each animal's pain, distress and activity levels were monitored and recorded for seven d following surgery.

Harvesting Tissue. Fourteen days after surgery, animals were weighed and anesthetized with 2-3% isoflurane and supplemental oxygen. The skin surrounding the ankle was removed and blunt dissection used to separate the fascia from skeletal muscle. The gastrocnemius (medial and lateral heads), plantaris, soleus and heart were harvested, immediately weighed and flash frozen in liquid nitrogen. Harvested muscles were stored in -80°C until analyzed.

Blood Sample. A 2 mL blood sample was drawn from each animal during tissue harvesting and placed in cooled EDTA vacutainers. Blood samples were centrifuged at 3000 rpm for 15 min at 3°C and the plasma separated and stored in -80°C until analyzed.

ELISA. Total plasma myostatin concentrations were measured using an antibody sandwich enzyme-linked immunosorbent assay (ELISA) kit (Quantikine: R&D Systems Minneapolis, MN). To isolate active plasma myostatin, plasma samples were filtered through a 30 kD Micro Bio-Spin Chromatography Column (Bio-Rad Laboratories, Inc., Hercules, CA). The filtering of these plasma samples resulted in a retention of the larger latent and precursor myostatin proteins in the column but allowed the smaller (26 kD) active myostatin molecule to be collected in the filtrate. Circulating inactive myostatin was estimated by subtracting the measurement of active myostatin protein from the measurement of total myostatin in plasma.

Homogenization. Whole muscle samples were powdered with mortar and pestle under liquid nitrogen. Approximately 50 mg of powered muscle was then homogenized (9 ml/mg) on ice 2 x 30 sec in a homogenization buffer (50 mM tris-HCL, pH 7.4; 250 mM mannitol; 50 mM

NaF; 5 mM sodium pyrophosphate; 1 mM EDTA; 1 mM EGTA; 1% Triton X-100; 50 mM β-glycerophosphate; 1mM sodium orthovanadate; 1 mM DTT; 1 mM benzamidine; 0.1 mM phenylmethane sulfonyl fluoride; 5 µg/ml soybean trypsin inhibitor) containing a protease inhibitor mix (1 M DTT (dithiothrietol), 1 M benzamidine, 5 ug/ul STI (soybean trypsin inhibitor), 200 mM Na_3Vo_4 (sodium orthovanadate), 200 mM PMSF (phenylmethane sulfonyl fluoride)). Homogenates then underwent three cycles of freeze/thaw lysis, after which they were centrifuged at 16,000 x g for 10 min at 4°C. Total protein concentration of the supernatant was determined and the supernatant was aliqouted into eppendorf tubes and stored at -80°C until analysis.

Total Protein Analysis. Total protein concentration of homogenates was determined using a DC (detergent compatible) Protein Assay (DC Protein Assay Kit, Bio-Rad Laboratories, Inc., Hercules, CA). Absorbance was measured on a micro plate reader (VICTOR3, PerkinElmer and Analytical Sciences, Shelton, CT) at a wavelength of 750 nm.

Western Blotting. Samples were electrophoresed under reducing conditions by adding 5% β-mercaptoethanol to sample buffer and boiling samples for 10 min. Each homogenate was loaded into the wells of a 12% TGX Criterion gel (Bio-Rad Laboratories, Inc., Hercules, CA) at a total protein content of 40 ug. Treatment and sham samples of each animal were loaded into neighboring lanes of the same gel. Proteins were separated at 200 V for 50 min. A molecular weight ladder (Precision Plus Protein All Blue Standards, Bio-Rad Laboratories, Inc., Hercules, CA) and 50 ug of a positive control (*Myostatin:* Recombinant Human/Mouse/Rat GDF-8/Myostatin R&D Systems, Inc., Minneapolis, MN. *BMP-1:* NIH/3T3 Whole Cell Lysate Santa Cruz Biotechnology Inc., Santa Cruz, CA) were included on each gel.

Transfer. Proteins were electrotransferred onto a polyvinylidene difluoride (PVDF) membrane in chilled Tris/Glycine transfer buffer for 1 h at 100 volts. Protein transfer to membrane was confirmed with a Ponceau S Stain.

Myostatin (GDF-8). Membranes were first blocked in 3% BSA (bovine serum albumin) in TBS-T (TBS pH 7.4 + 0.1% Tween-20) for 1 h. They were then incubated in primary antibody; a polyclonal goat IgG (AF788, R&D Systems, Inc., Minneapolis, MN) diluted *1:1000* in 0.1% BSA in TBS-T for 1 h (13). The AF788 antibody targets the carboxy-terminal region (Asp268-Ser376) of the myostatin molecule and therefore is able to identify all three forms of the protein (precursor, latent, and active myostatin) in skeletal muscle (13). Membranes were rinsed vigorously twice for 15 min with TBS-T. Lastly, they were incubated in a goat IgG Horseradish Peroxidase-conjugated secondary antibody, diluted *1:5000* in TBS-T for 30 min. All steps were performed at room temperature.

BMP-1. Membranes were blocked 1 h in 5% non-fat dry milk in TBS-T (TBS pH 7.6 + 0.1% Tween-20). They were incubated 1 h in primary antibody; a rabbit polyclonal [BMP-1 (H-300), Santa Cruz Biotechnology Inc., Santa Cruz, CA)] diluted *1:200* in 1% milk in TBS-T. Membranes were rinsed vigorously three times, 5 min each in TBS-T. Lastly, they were incubated in secondary antibody; a goat anti-rabbit IgG-HRP (Santa Cruz Biotechnology Inc., Santa Cruz, CA) diluted *1:4000* in 1% milk in TBS-T for 45 min. All steps were performed at room temperature.

GAPDH. GAPDH was measured on each membrane as a loading control. Previously incubated gels were stripped with an 8 min incubation in stripping buffer (0.2 M glycine, 10% tween, 0.1% SDS, pH 2.2) at 37°C, one 5 min wash at room temperature in TBS-T, another 8 min incubation in 0.2 M NaOH at 37°C, then followed by 2 x 5 min washes in TBS-T at room

temperature. Once previous bound antibodies were stripped, the membranes were blocked in 3% BSA for 1 h at room temperature and then incubated 1 h in primary antibody; a goat polyclonal [GAPDH (I-19), Santa Cruz Biotechnology Inc., Santa Cruz, CA)] diluted *1:10,000* in 0.1% BSA in TBS-T. Following primary incubation, the gel was rinsed three times, 5 min each in TBS-T and incubated in a rabbit anti-goat IgG-HRP secondary antibody (Santa Cruz Biotechnology Inc., Santa Cruz, CA) diluted *1:30,000* in 0.1% BSA in TBS-T for 30 min at room temperature.

Analysis. Chemiluminescence detection solution was applied to each blot and incubated for 5 min according to the manufacturer's instructions (Clarity Western ECL Substrate, Bio-Rad Laboratories, Inc., Hercules, CA). An image of each blot was then taken using a ChemiDoc XRS CCD camera-based imager (Bio-Rad Laboratories, Inc., Hercules, CA). Quantitative protein analysis of each band was performed using the Quantity One Software version 4.6.5 (Bio-Rad Laboratories, Inc., Hercules, CA). Samples were run in duplicate on separate gels and the two measurements were averaged and then normalized to the expression of GAPDH.

Statistical Analysis. Standard statistical procedures were used to calculate the means and standard errors. A paired t-test was used to compare specific protein levels in treatment and sham legs of each animal. An analysis of variance (ANOVA) was used to compare plasma myostatin measurements of animals that received the overload treatment and cage control animals. Animal wheel-running activity pre- and postsurgery was analyzed using a Dunnett's test. Results were presented as mean ± SEM. Differences between the means were regarded as significant when a value of $p < 0.05$ was obtained.

RESULTS

Figure 1 illustrates the free wheel-running behavior of the rats 5 d prior and 14 d post-tenotomy. Rats typically increased their running distance per day when first placed in the individual cages containing the running wheels. On the day just prior to tenotomy surgery (day^{-1}, Figure 1) animals ran an average distance of 4750.7 ± 552.5 m. Following tenotomy surgery, the daily running distance dropped significantly but returned to distances seen prior to tenotomy by day 4 and by day 14 post-tenotomy animals ran an average distance of 5491.09 ± 665.96 m.

The overloaded muscles showed significant hypertrophy as shown in Figure 2. Following two weeks of overload both the plantaris (494 ± 29 vs. 405 ± 15 mg, $p < 0.05$) and soleus (289 ± 12 vs. 179 ± 37 mg, $p < 0.05$) muscles increased in weight while the gastrocnemius weight on the tenotomy leg atrophied ($p < 0.05$).

Overloaded soleus and plantaris skeletal muscle reduced the concentration of active myostatin protein by 32.7 ± 9.4% and 28.5 ± 8.5%, respectively ($p < 0.01$, Figure 3). Latent myostatin protein also decreased by 15.0 ± 5.9% and 7.0 ± 2.3% ($p < 0.05$) in overloaded soleus and plantaris muscle, respectively. Precursor myostatin protein concentration was reduced 17.5 ± 5.9% in the overloaded plantaris muscle ($p < 0.05$) and was unchanged in overloaded soleus muscle.

Following 14 d of overload, the soleus and plantaris muscles decreased levels of the proteinase BMP-1 by 40.4 ± 12.9% and 32.9 ± 6.9% ($p < 0.01$, Figure 4), respectively.

Circulating plasma myostatin levels are shown in Figure 5. Plasma concentrations of total and active myostatin proteins were similar in overloaded and control animals and averaged 8865 ± 526 pg/ml and 569 ± 28 pg/ml, respectively. In plasma, active myostatin represented 6.5 ± 0.2% of the total circulating myostatin.

DISCUSSION

Myostatin is located in two pools: the extracellular matrix of skeletal muscle (local pool) and circulating in the blood (systemic pool) (3, 21, 40). Regulation of the myostatin protein during muscle growth, in either of these locations, is not fully understood. Using an overload model, we measured myostatin protein levels to better understand regulation of the myostatin protein during muscle growth.

Following overload-induced skeletal muscle growth, concentrations of all forms of local myostatin (precursor, latent and active) were decreased when compared to the nonoverloaded muscle. In addition, the proteinase regulator that converts the myostatin latent complex to its active form, BMP-1, was reduced in overloaded skeletal muscles. These data indicate a general reduction in levels of myostatin proteins during overload-induced skeletal muscle hypertrophy and a reduction in the capacity to convert latent myostatin complex into its active form by BMP-1.

Myostatin is expressed in the precursor form and proteolytically processed into the latent and active protein forms. Conversion to latent myostatin is the first posttranslational modification and is necessary for downstream signaling (19). Previous studies have shown that processing of precursor myostatin is a key regulatory step in the myostatin signaling pathway and occurs in the bloodstream and in the muscle (3, 23). Levels of precursor myostatin were significantly decreased in overloaded plantaris muscle (Figure 3) and tended to be reduced in overloaded soleus muscle when compared to control muscles. These results confirm the findings of Anderson et al. (3) and McFarlane et al. (23) demonstrating that the precursor protein is one point in the pathway where muscle myostatin is regulated during muscle growth. More

importantly, our data demonstrate this regulatory pathway is operating during functional overload in adult skeletal muscle.

The latent form of the myostatin protein is a second point of protein regulation. Latent myostatin is a complex consisting of the active protein and a propeptide. Myostatin is inactive in the latent form and receptor binding does not occur until the propeptide is removed. Several factors which cleave the propeptide *in vitro* include heat, alkali or acid. However, *in vivo*, cleavage can occur via extracellular matrix proteinases (37). Animals with higher concentrations of circulating latent myostatin have greater muscle mass (19, 39). Lee et al. (21) altered the myostatin gene of a mouse resulting in the production of a propeptide that could not be cleaved by extracellular matrix proteinases in the BMP-1/TLD family (21). These animals exhibited significant muscle hypertrophy with increased amounts of circulating latent myostatin protein compared to wild type mice. These animals exhibited significant muscle hypertrophy with increased amounts of circulating latent myostatin protein compared to wild type mice. These authors concluded that the increased muscle mass was a result of a reduction in latent myostatin being cleaved to its active form. Latent myostatin in the muscle was however not measured in the transgenic animals. Based on the findings of Lee et al. we hypothesized that following an overload stimulus skeletal muscle latent myostatin would increase. Contrary to this hypothesis we show a decrease in latent myostatin in overloaded muscles (Figure 3). To our knowledge**,** no previous studies have measured skeletal muscle latent myostatin following overload-induced muscle growth. Therefore, these data appear to contribute new evidence of how the latent complex functions in the muscle during muscle growth.

Once the propeptide is removed from the latent complex, myostatin becomes an active protein (20). Active myostatin binds to target cell receptors and initiates a signaling cascade

inside the cell that inhibits muscle cell growth pathways (2). Active myostatin exerts its inhibitory effects in a concentration-dependent manner. As such, to increase skeletal muscle mass there must be a reduction in the amount of active myostatin (20). The majority of myostatin literature related to skeletal muscle growth is comprised of studies that measured myostatin mRNA expression. Our data show that active myostatin protein was significantly decreased (Figure 3) in overloaded plantaris and soleus muscles. These data provide further evidence that active myostatin protein levels are reduced during mechanical overload muscle growth, and suggests that reducing the amount of active myostatin protein at a muscle site may be one way to stimulate muscle growth in overloaded skeletal muscles.

Previous studies have provided evidence of myostatin functioning both systemically and locally (3, 4, 21). Increasing the amount of circulating myostatin causes muscle wasting throughout the body, indicating the protein's systemic effect (40). Lee et at. (21) reported that the majority of circulating myostatin protein in mice was in the latent form and suggested that the circulating form of myostatin was most important in regulating muscle growth (systemic effect). Anderson et al. (3) demonstrated that circulating myostatin is able to enter and accumulate in the muscle's extracellular matrix, and suggested that local mechanisms activate latent myostatin and eventually control individual muscle growth (local effect). We measured muscle and plasma myostatin levels in an effort to understand the relationship between circulating and muscle myostatin and its impact on muscle growth during functional overload. Based on the findings of previous studies, if muscle growth was regulated primarily by circulating myostatin then the amount of circulating latent myostatin should increase during functional overload (11, 21).

Total myostatin and active myostatin protein were measured in the plasma of animals following two weeks of unilateral hindlimb overload and compared to plasma measurements of

cage control animals that did not receive the overload treatment. We found no differences in plasma myostatin protein levels (Figure 5) in overloaded and control animals. It is possible that circulating myostatin levels only reflect myostatin leaking from muscle pools and have no regulatory role. Instead, during overload the effects of circulating myostatin are mediated locally at the muscle cell (20). Our data appear to support this speculation. However, it is also possible that the overload stimulus in our unilateral model was insufficient to produce significant changes in circulating myostatin levels.

A body of literature has demonstrated *in vitro* that all four proteinases of the bone morphogenetic protein-1/tolloid (BMP-1/Tolloid) family of metalloproteinases (BMP-1, mTLD, mTLL-1 and mTLL-2) cleave latent myostatin into the active protein (5, 37). However, identification of the specific proteinase or combined proteinases involved in this conversion process *in vivo* is unclear. Greenspan et al. (5) performed an analysis of the four proteinases' activity in neural, bone and skeletal muscle mammal tissues. Based on their findings, we concluded that the proteinase BMP-1 from the BMP-1/TLD family would be the proteinase in adult skeletal muscle responsible for regulating the conversion of latent myostatin to the active protein. Overloaded soleus and plantaris muscles showed significant reductions in the concentration of the proteinase BMP-1 (Figure 4). As previously discussed, active myostatin protein also decreased in the overloaded muscles. These measurements together provide evidence of an association between the proteinase BMP-1 and the amount of active myostatin in an individual muscle. The data presented here supports the idea that both myostatin pools, systemic and local, are regulated locally at the muscle cell level. In addition, reduced activity of the proteinase BMP-1, found in the in the extracellular matrix, contributes to local myostatin regulation.

It has previously been demonstrated that myostatin mRNA expression decreases in an overload model (38) and increases with unloading (1, 33). However, transcription data only roughly describes protein activity and changes at the gene expression level are not always correlated with changes in protein concentration (32). This may be especially true for the myostatin protein pathway because the active myostatin protein accounts for only 6.5% of the total circulating myostatin and undergoes several posttranslational modifications before becoming active. Current literature suggests that myostatin protein modifications are part of a complex regulatory system. Myostatin is released from the producing cell and distributed to individual muscles via circulation. Currently, the regulation of myostatin involved in the growth of individual muscles is not fully understood. Two theories have been presented: regulation of circulating myostatin and regulation of muscle myostatin.

This study examines the distribution of myostatin proteins, active, latent and precursor, in muscle and plasma following two weeks of overload-induced adult muscle growth. Our data demonstrates decreased concentrations of precursor, latent and active myostatin in overloaded muscles with no change in total, latent and active circulating myostatin. Based on these data, it appears that the myostatin signaling pathway in overloaded muscles is generally downregulated and contributes to muscle hypertrophy. Our data show decreased concentrations of BMP-1 and active myostatin in overloaded muscles. This supports the concept of local control of posttranslational modification of myostatin in regulating muscle growth during functional overload. Based on these observations, it appears that local targeting of posttranslational myostatin protein may be one way to increase muscle growth of individual muscles during states of disease, disuse and aging.

REFERENCES

1. **Adams GR, Haddad F, Bodell PW, Tran PD, and Baldwin KM**. Combined isometric, concentric, and eccentric resistance exercise prevents unloading-induced muscle atrophy in rats. *J Appl Physiol* 103: 1644-1654, 2007.

2. **Amirouche A, Durieux AC, Banzet S, Koulmann N, Bonnefoy R, Mouret C, Bigard X, Peinnequin A, and Freyssenet D**. Down-regulation of Akt/mammalian target of rapamycin signaling pathway in response to myostatin overexpression in skeletal muscle. *Endocrinology* 150: 286-294, 2009.

3. **Anderson SB, Goldberg AL, and Whitman M**. Identification of a novel pool of extracellular pro-myostatin in skeletal muscle. *J Biol Chem* 283: 7027-7035, 2008.

4. **Breitbart A, Auger-Messier M, Molkentin JD, and Heineke J**. Myostatin from the heart: local and systemic actions in cardiac failure and muscle wasting. *Am J Physiol Heart Circ Physiol* 300: H1973-1982, 2011.

5. **Ge G and Greenspan DS**. Developmental roles of the BMP1/TLD metalloproteinases. *Birth defects Res., Part C* 78: 47-68, 2006.

6. **Goldberg AL**. Protein synthesis during work-induced growth of skeletal muscle. *J Cell Biol* 36: 653-658, 1968.

7. **Goldberg AL**. Protein turnover in skeletal muscle. I. Protein catabolism during work-induced hypertrophy and growth induced with growth hormone. *J Biol Chem* 244: 3217-3222, 1969.

8. **Goldberg AL**. Work-induced growth of skeletal muscle in normal and hypophysectomized rats. *Am J Physiol* 213: 1193-1198, 1967.

9. **Goldberg AL and Goodman HM**. Amino acid transport during work-induced growth of skeletal muscle. *Am J Physiol* 216: 1111-1115, 1969.

10. **Goldspink DF, Garlick PJ, and McNurlan MA**. Protein turnover measured in vivo and in vitro in muscles undergoing compensatory growth and subsequent denervation atrophy. *Biochem J* 210: 89-98, 1983.

11. **Hill JJ, Davies MV, Pearson AA, Wang JH, Hewick RM, Wolfman NM, and Qiu Y**. The myostatin propeptide and the follistatin-related gene are inhibitory binding proteins of myostatin in normal serum. *J Biol Chem* 277: 40735-40741, 2002.

12. **Hittel DS, Axelson M, Sarna N, Shearer J, Huffman KM, and Kraus WE**. Myostatin decreases with aerobic exercise and associates with insulin resistance. *Med Sci Sports Exerc* 42: 2023-2029, 2010.

13. **Hittel DS, Berggren JR, Shearer J, Boyle K, and Houmard JA**. Increased secretion and expression of myostatin in skeletal muscle from extremely obese women. *Diabetes* 58: 30-38, 2009.

14. **Hulmi JJ, Ahtiainen JP, Kaasalainen T, Pollanen E, Hakkinen K, Alen M, Selanne H, Kovanen V, and Mero AA**. Postexercise myostatin and activin IIb mRNA levels: effects of strength training. *Med Sci Sports Exerc* 39: 289-297, 2007.

15. **Kovacheva EL, Hikim AP, Shen R, Sinha I, and Sinha-Hikim I**. Testosterone supplementation reverses sarcopenia in aging through regulation of myostatin, c-Jun NH2-terminal kinase, Notch, and Akt signaling pathways. *Endocrinology* 151: 628-638, 2010.

16. **Lakshman KM, Bhasin S, Corcoran C, Collins-Racie LA, Tchistiakova L, Forlow SB, St Ledger K, Burczynski ME, Dorner AJ, and Lavallie ER**. Measurement of myostatin concentrations in human serum: Circulating concentrations in young and older men and effects of testosterone administration. *Mol Cell Endocrinol* 302: 26-32, 2009.

17. **Langley B, Thomas M, Bishop A, Sharma M, Gilmour S, and Kambadur R**. Myostatin inhibits myoblast differentiation by down-regulating MyoD expression. *J Biol Chem* 277: 49831-49840, 2002.

18. **Laurent GJ and Millward DJ**. Protein turnover during skeletal muscle hypertrophy. *Federation proceedings* 39: 42-47, 1980.

19. **Lee S-J**. Regulation of muscle mass by myostatin. *Annual Review Of Cell And Developmental Biology* 20: 61-86, 2004.

20. **Lee S-J**. Extracellular regulation of myostatin: A molecular rheostat for muscle mass. *Immunology, endocrine & metabolic agents in medicinal chemistry* 10: 183-194, 2010.

21. **Lee S-J**. Genetic analysis of the role of proteolysis in the activation of latent myostatin. *PLoS One* 3: e1628, 2008.

22. **Lee S-J and McPherron AC**. Regulation of myostatin activity and muscle growth. *Proc Natl Acad Sci U.S.A.* 98: 9306-9311, 2001.

23. **McFarlane C, Langley B, Thomas M, Hennebry A, Plummer E, Nicholas G, McMahon C, Sharma M, and Kambadur R**. Proteolytic processing of myostatin is auto-regulated during myogenesis. *Dev Biol* 283: 58-69, 2005.

24. **McPherron AC, Lawler AM, and Lee S-J**. Regulation of skeletal muscle mass in mice by a new TGF-beta superfamily member. *Nature* 387: 83-90, 1997.

25. **McPherron AC and Lee S-J**. Double muscling in cattle due to mutations in the myostatin gene. *Proc Natl Acad Sci U.S.A.* 94: 12457-12461, 1997.

26. **Miyazono K, Ichijo H, and Heldin CH**. Transforming growth factor-beta: Latent forms, binding proteins and receptors. *Growth Factors* 8: 11-22, 1993.

27. **Rebbapragada A, Benchabane H, Wrana JL, Celeste AJ, and Attisano L**. Myostatin signals through a transforming growth factor beta-like signaling pathway to block adipogenesis. *Mol Cell Biol* 23: 7230-7242, 2003.

28. **Roth SM, Martel GF, Ferrell RE, Metter EJ, Hurley BF, and Rogers MA**. Myostatin gene expression is reduced in humans with heavy-resistance strength training: A brief communication. *Exp Biol Med (Maywood)* 228: 706-709, 2003.

29. **Schuelke M, Wagner KR, Stolz LE, Hubner C, Riebel T, Komen W, Braun T, Tobin JF, and Lee S-J**. Myostatin mutation associated with gross muscle hypertrophy in a child. *N Engl J Med* 350: 2682-2688, 2004.

30. **Thies RS, Chen T, Davies MV, Tomkinson KN, Pearson AA, Shakey QA, and Wolfman NM**. GDF-8 propeptide binds to GDF-8 and antagonizes biological activity by inhibiting GDF-8 receptor binding. *Growth Factors* 18: 251-259, 2001.

31. **Tsuchida K, Nakatani M, Uezumi A, Murakami T, and Cui X**. Signal transduction pathway through activin receptors as a therapeutic target of musculoskeletal diseases and cancer. *Endocrine J* 55: 11-21, 2008.

32. **Vogel C and Marcotte EM**. Insights into the regulation of protein abundance from proteomic and transcriptomic analyses. *Nat Rev Genet* 13: 227-232, 2012.

33. **Wehling M, Cai B, and Tidball JG**. Modulation of myostatin expression during modified muscle use. *FASEB J* 14: 103-110, 2000.

34. **Welle S, Bhatt K, Pinkert CA, Tawil R, and Thornton CA**. Muscle growth after postdevelopmental myostatin gene knockout. *Am J Physiol Endocrinol Metab* 292: E985-991, 2007.

35. **Welle S, Burgess K, Thornton CA, and Tawil R**. Relation between extent of myostatin depletion and muscle growth in mature mice. *Am J Physiol Endocrinol Metab* 297: E935-940, 2009.

36. **Whittemore LA, Song K, Li X, Aghajanian J, Davies M, Girgenrath S, Hill JJ, Jalenak M, Kelley P, Knight A, Maylor R, O'Hara D, Pearson A, Quazi A, Ryerson S, Tan XY, Tomkinson KN, Veldman GM, Widom A, Wright JF, Wudyka S, Zhao L, and Wolfman NM**. Inhibition of myostatin in adult mice increases skeletal muscle mass and strength. *Biochem Biophys Res Commun* 300: 965-971, 2003.

37. **Wolfman NM, McPherron AC, Pappano WN, Davies MV, Song K, Tomkinson KN, Wright JF, Zhao L, Sebald SM, Greenspan DS, and Leet SI**. Activation of latent myostatin by the BMP-1/tolloid family of metalloproteinases. *P Natl Acad Sci USA* 100: 15842-15846, 2003.

38. **Yamaguchi A, Fujikawa T, Shimada S, Kanbayashi I, Tateoka M, Soya H, Takeda H, Morita I, Matsubara K, and Hirai T**. Muscle IGF-I Ea, MGF, and myostatin mRNA expressions after compensatory overload in hypophysectomized rats. *Pflugers Arch* 453: 203-210, 2006.

39. **Yang J, Ratovitski T, Brady JP, Solomon MB, Wells KD, and Wall RJ**. Expression of myostatin pro domain results in muscular transgenic mice. *Mol Reprod Dev* 60: 351-361, 2001.

40. **Zimmers TA, Davies MV, Koniaris LG, Haynes P, Esquela AF, Tomkinson KN, McPherron AC, Wolfman NM, and Lee S-J**. Induction of cachexia in mice by systemically administered myostatin. *Science* 296: 1486-1488, 2002.

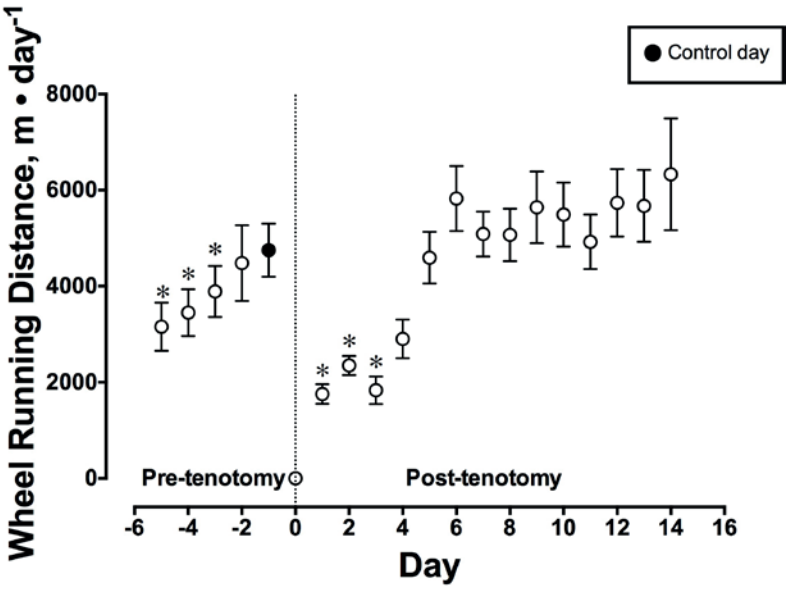

Figure 1. Average daily wheel-running distances 5 d prior and 14 d post-tenotomy surgery. Values expressed as mean ± 1 SEM, n = 11. *$p < 0.05$ different from control day (day^{-1}).

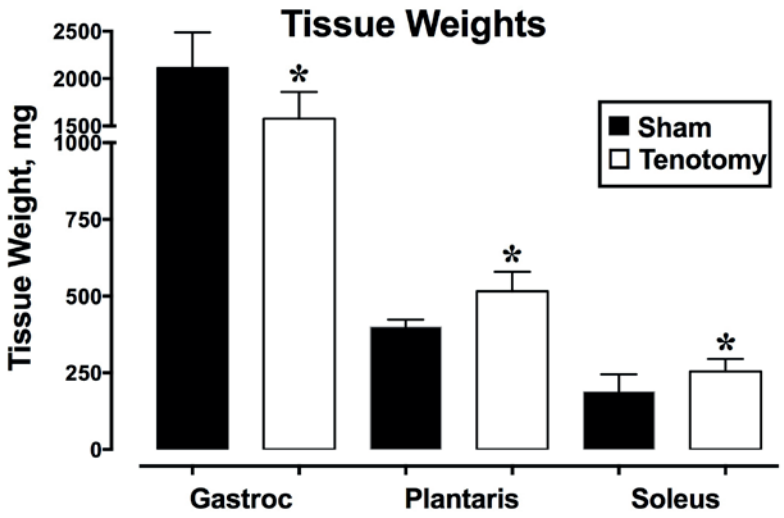

Figure 2. Wet weights of harvested skeletal muscle tissue two weeks post-tenotomy surgery. Values are expressed as mean ± SEM, n = 11. *p < 0.05 different from sham.

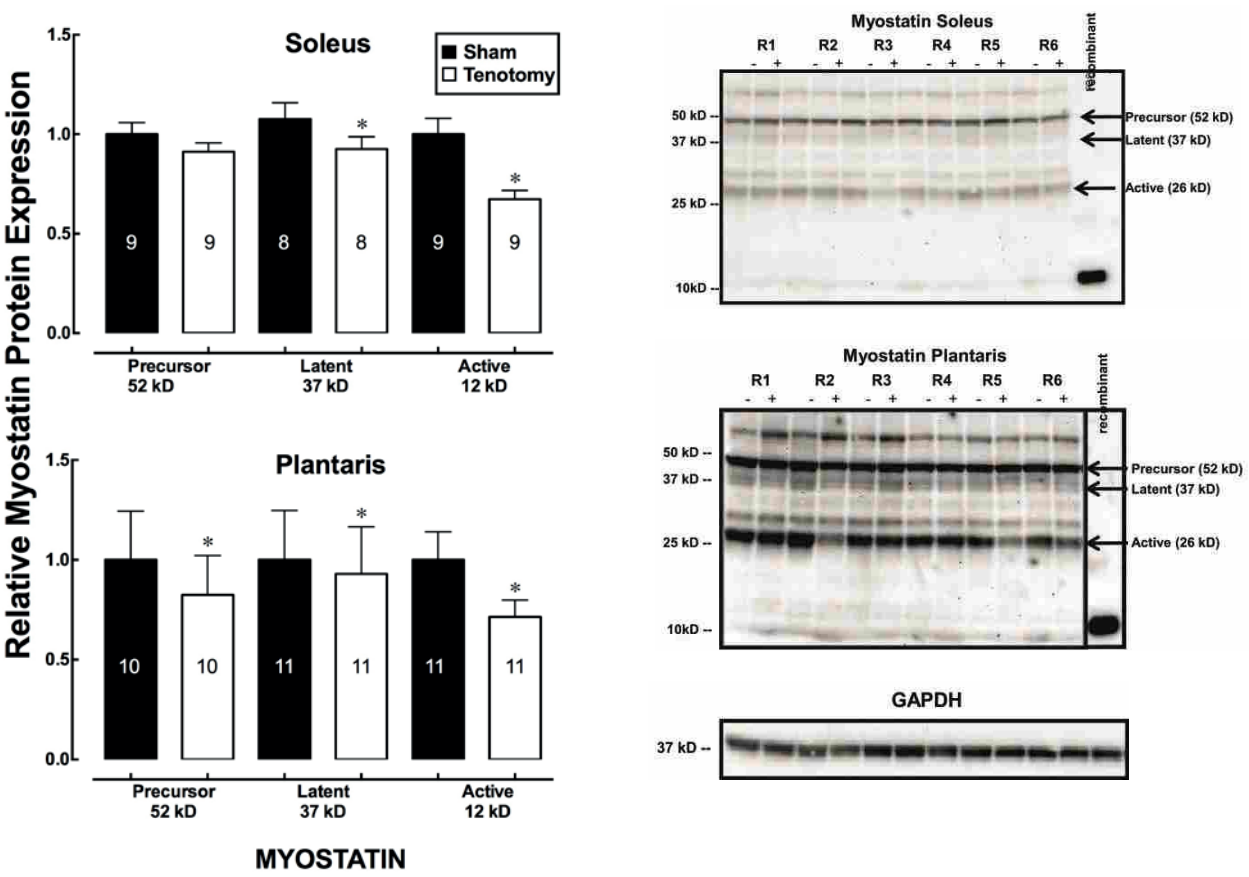

Figure 3. Relative myostatin protein levels in sham and overloaded soleus and plantaris muscles two weeks post-tenotomy surgery. Protein levels normalized to GAPDH levels and sham myostatin levels. Values are expressed as mean ± SEM. Sample size shown for each condition. *$p < 0.05$ different from sham. Representative Western blots for myostatin precursor, latent and active proteins in overloaded (+) and sham (-) soleus and plantaris muscles of six animals. GAPDH protein was analyzed and used as a loading control.

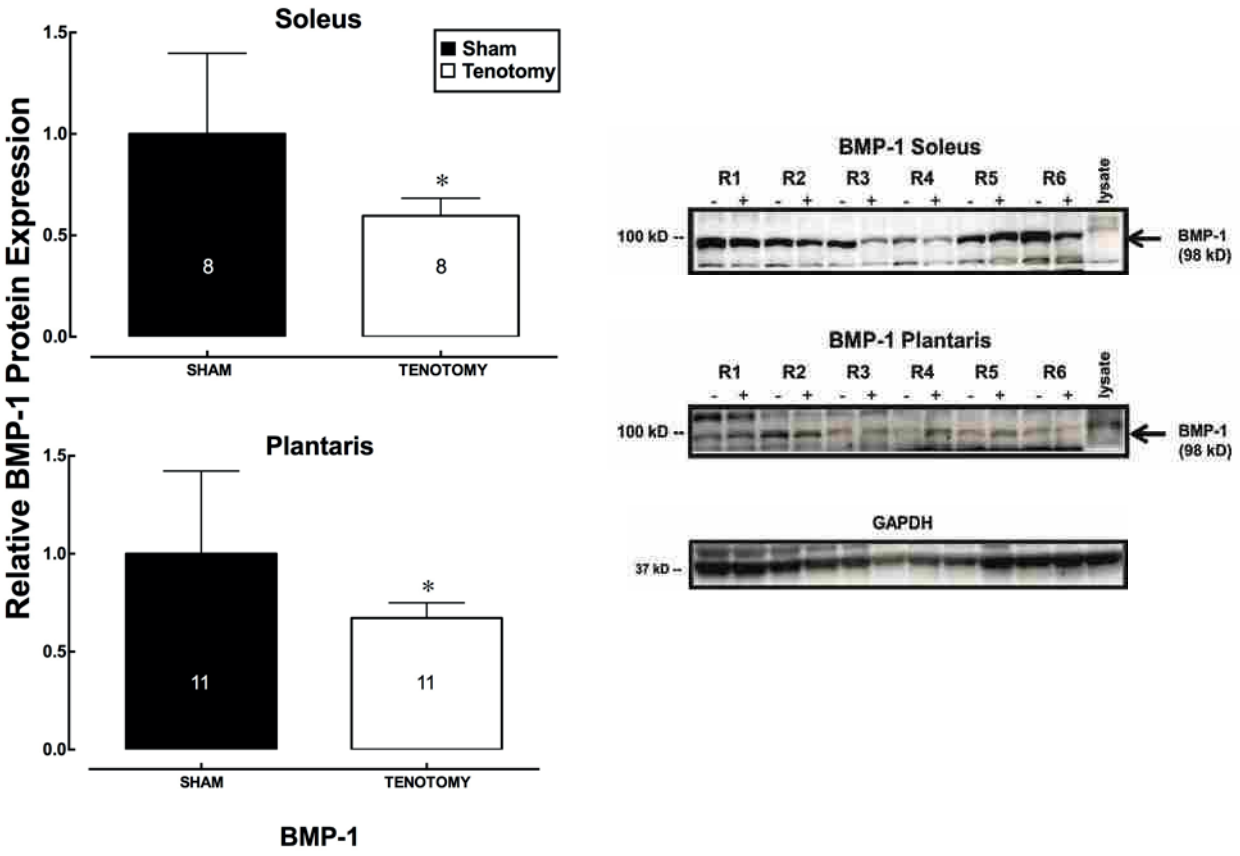

Figure 4. Relative BMP-1 protein levels in sham and overloaded soleus and plantaris muscles two weeks post-tenotomy surgery. Protein levels normalized to GAPDH levels and sham BMP-1 levels. Values are expressed as mean ± SEM. Sample size shown for each condition. *$p < 0.05$ different from sham. Representative Western blots for BMP-1 protein in overloaded (+) and sham (-) soleus and plantaris muscles of six animals. GAPDH protein was analyzed and used as a loading control.

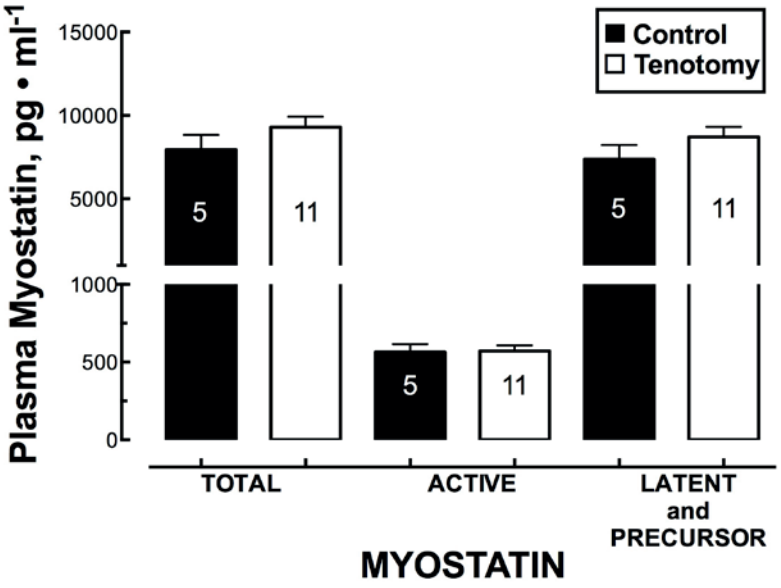

Figure 5. Plasma myostatin protein concentrations ($pg \cdot ml^{-1}$) in control (n = 5) and overloaded animals (n = 11). Values are mean ± SEM.